Accepted Manuscript

Characterisation of the TNF superfamily members CD40L and BAFF in the small-spotted catshark (*Scyliorhinus canicula*)

Ronggai Li, Anthony K. Redmond, Tiehui Wang, Steve Bird, Dr. Helen Dooley, Chris J. Secombes

PII: S1050-4648(15)30158-3

DOI: 10.1016/j.fsi.2015.09.033

Reference: YFSIM 3621

To appear in: *Fish and Shellfish Immunology*

Received Date: 21 July 2015

Revised Date: 8 September 2015

Accepted Date: 15 September 2015

Please cite this article as: Li R, Redmond AK, Wang T, Bird S, Dooley H, Secombes CJ, Characterisation of the TNF superfamily members CD40L and BAFF in the small-spotted catshark (*Scyliorhinus canicula*), *Fish and Shellfish Immunology* (2015), doi: 10.1016/j.fsi.2015.09.033.

Characterisation of the TNF superfamily members CD40L and BAFF in the small-spotted catshark (*Scyliorhinus canicula*).

Ronggai Li[1†], Anthony K. Redmond[2], Tiehui Wang[1], Steve Bird[3], Helen Dooley[1] & Chris J. Secombes[1].

[1]Scottish Fish Immunology Research Centre (SFIRC), School of Biological Sciences, University of Aberdeen, Aberdeen AB24 2TZ, United Kingdom. [2]Centre for Genome-Enabled Biology & Medicine (CGEBM), University of Aberdeen, Aberdeen AB24 2TZ, United Kingdom. [3]Department of Biological Sciences, School of Science and Engineering, University of Waikato, New Zealand.

[†]Current address: Crop Genetics & Breeding Laboratory of Hebei Province/Institute of Cereal and Oil Crops, Hebei Academy of Agriculture and Forestry Sciences, 050035 Shijiazhuang, China.

Corresponding author: Dr Helen Dooley. School of Biological Sciences, Zoology Building, Tillydrone Avenue, University of Aberdeen, Aberdeen AB24 2TZ, United Kingdom.

Tel: +44-1224-274460. Email: h.dooley@abdn.ac.uk

Abstract

The tumour necrosis factor superfamily (TNFSF) members CD40L and BAFF play critical roles in mammalian B cell survival, proliferation and maturation, however little is known about these key cytokines in the oldest jawed vertebrates, the cartilaginous fishes. Here we report the cloning of CD40L and BAFF orthologues (designated ScCD40L and ScBAFF) in the small-spotted catshark (*Scyliorhinus canicula*). As predicted both proteins are type II membrane-bound proteins with a TNF homology domain in their extracellular region and both are highly expressed in shark immune tissues. ScCD40L transcript levels correlate with those of TCRα and transcription of both genes is modulated in peripheral blood leukocytes following *in vitro* stimulation. Although a putative CD40L orthologue was identified in the elephant shark genome the work herein is the first molecular characterisation and transcriptional analysis of CD40L in a cartilaginous fish. ScBAFF was also cloned and its transcription characterised in an attempt to resolve the discrepancies observed between spiny dogfish BAFF and bamboo shark BAFF in previously published studies.

Keywords: CD40L; BAFF; TNFSF; shark; cartilaginous fish.

Abbreviations: BCMA, B cell maturation antigen; TACI, transmembrane activator and calcium signal–modulating cyclophilin ligand interactor; THD, TNF homology domain; TLR, Toll-like receptor; LPS, lipopolysaccharide; PHA, phytohaemagglutinin; PMA, phorbol 12-myristate 13-acetate, PWM, pokeweed mitogen; polyI:C, polyinocinic:polycytidylic acid.

1. Introduction

In mammals, a number of tumour necrosis factor superfamily (TNFSF) members and their receptors (TNFRSF) are important regulators of B cell development and functioning [1]. TNFSF members are type II transmembrane proteins typified by the presence of a conserved TNF homology domain (THD) in their extracellular C-terminus. The THD is composed of ten β-strands, which fold to form a classical 'jellyroll' topology. While the majority of these are expressed as membrane-bound proteins many contain a proteolytic cleavage site which releases a soluble form [1]. Structurally each TNFSF molecule is a conical trimer, formed from three monomers [2-5], which binds its associated receptor(s) to initiate downstream signalling events.

The TNFSF member CD40L (also known as CD154 or TNFSF5) was initially identified as a cell-surface protein on activated T cells. However it is now apparent that CD40L is also present on a wide range of other mammalian cell types including activated B cells, monocytes, macrophages, dendritic cells, endothelial cells and platelets [6]. The classical receptor for CD40L is the type I membrane protein CD40 (also known as TNFRSF5) which was first identified on B cells. In addition, other receptors for CD40L have recently been identified, namely αIIbβ3, αMβ2 (also called Mac-1) and α5β1 integrins [7-9], suggesting additional immunomodulatory functions. The interaction of CD40/CD40L is well established as an immune mediator in mammals, particularly in the promotion of T-dependent B cell responses including B cell proliferation, differentiation, immunoglobulin (Ig) production and Ig isotype class switching [10-12]. The interaction of this pair also up-regulates other costimulatory molecules (such as CD54, CD58/LFA-3, CD80/B7-1, CD86/B7-2) and promotes the production of cytokines such as TNF-α, IFN-α, IL-8, IL-10 and IL-12, which are important in the induction of innate and adaptive immune responses [13].

BAFF (also known as TNFSF13B, BLyS or TALL-1) is mainly expressed on the surface of innate immune cells (monocytes, dendritic cells and macrophages) and activated T cells [14;15]. However, it can be processed to a soluble form by proteolytic cleavage at a furin consensus site in the C-terminal extracellular domain, with both the membrane-bound and soluble forms being biologically active [14]. Soluble BAFF adopts the usual trimeric form of the TNFSF, but it is the only member of the family thought to further assemble into an ordered structure containing twenty trimers (i.e. a 60-mer) [16]. The crystal structure of

soluble BAFF reveals an unusually long and flexible D-E loop compared to other TNFSF members, which dictates receptor binding specificity and confers the ability to form this virus-like multimer [2;16]. In mammals BAFF exerts its effect by binding to one of three receptors, preferentially the BAFF receptor (BAFF-R or TNFRSF13C) but also, with lower affinity, to the receptors BCMA (TNFRSF17) and TACI (TNFRSF13B) [17]. Notably a closely related TNFSF ligand called APRIL (TNFSF13) also binds the same receptors as BAFF but with a different specificity; APRIL binds with highest affinity to BCMA and with lower affinity to TACI (and, potentially, weakly to BAFF-R) [18], the interaction being aided by the oligomerisation of APRIL following its binding to sulphated glycosaminoglycans [19]. Both BAFF and APRIL are critical for B cell survival and differentiation however they act at different points in B cell development; antigen naïve B cells rely mainly upon BAFF signalling for their survival while antigen-experienced B cells require APRIL [20].

It is now widely accepted that an adaptive immune system based upon Igs, T cell receptors (TCRs) and major histocompatibility complex (MHC) molecules was established sometime before cartilaginous fish emerged from the common ancestor with other jawed vertebrates ~450 million years ago [21]. It is apparent that cartilaginous fish can generate a robust, antigen-specific, antibody response following immunological challenge [22;23]. However, little is known of the processes involved in the development, maintenance or proliferation of cartilaginous fish B cells, mainly because most of the required molecules have yet to be characterised in this lineage. While a putative gene for CD40L has recently been identified in the genome of the elephant shark (*Callorhinchus milii*; a chimera) [24] this molecule has yet to be properly characterised in any cartilaginous fish species. Additionally although BAFF orthologues have recently been cloned from the spiny dogfish (*Squalus acanthias*) and white-spotted bamboo shark (*Chiloscyllium plagiosum*) these studies showed that dogfish BAFF has an additional exon that extends the 'elbow' region of the molecule [25;26]. This exon is lacking in bamboo shark BAFF as well as that of other vertebrate species. The tissue expression pattern of BAFF also differed considerably between the two shark species.

Herein we describe the cloning of CD40L from the small-spotted catshark (*Scyliorhinus canicula*) and, for the first time, characterise the transcription profile of this molecule in a range of catshark tissues as well as in peripheral blood leukocytes (PBLs) stimulated *in vitro*

with a range of mitogens and PAMPs. Additionally we cloned BAFF from catshark, characterised its transcription, and performed robust phylogenetic analysis in an attempt to resolve the discrepancies observed between spiny dogfish BAFF and bamboo shark BAFF in previous studies.

2. Materials and methods

2.1. Small-spotted catshark

Sexually mature, wild-caught, small-spotted catsharks (weighing 600-1100 g) were collected from the North Sea and maintained in 1 m-diameter tanks supplied with flow-through seawater at 8-12°C, in the University of Aberdeen aquarium facility. Animals were anaesthetised with MS222 (0.12g/L seawater) prior to any procedure. Blood samples were taken from the caudal vein and stored on ice prior to the isolation of peripheral blood lymphocytes (PBLs). Peripheral blood and tissues from four catsharks were used for primary cell culture experiments and tissue expression analysis. All procedures were conducted in accordance with the UK Home Office 'Animals (Scientific Procedures) Act 1986 Amendment Regulations 2012' on animal care and use.

2.2. RNA isolation and cDNA synthesis

Total RNA was extracted from harvested tissues or PBLs using TRIzol reagent (Invitrogen) as described previously [25]. Briefly, tissues were mechanically disrupted in TRIzol reagent (Invitrogen, UK) with the subsequent addition of 1/5 volume of chloroform. Following centrifugation at 4°C the upper phase was transferred to an RNase-free tube and the RNA precipitated by the addition of isopropanol. After centrifugation the resultant RNA pellet was washed twice with 75% ethanol, re-centrifuged to pellet the RNA, any remaining ethanol aspirated and the pellet allowed to air dry. The RNA pellets were then resuspended in an appropriate volume of RNase-free H_2O and stored at -80°C for future use. For gene cloning cDNA was synthesised using a SMART cDNA synthesis kit (Clontech) following the manufacturer's protocol. For real-time RT-PCR analysis of gene expression, the RNA pellet was re-dissolved in 32µl of oligo(dT)28VN (2 mM), then converted to cDNA using RevertAid Reverse Transcriptase (Thermo Scientific). The generated cDNA was diluted with 300 µl of

TE buffer (10 mMTris–HCl, 1 mM EDTA, pH 7.5) and stored at -20 °C ready for use in real-time PCR.

2.3. Gene cloning and sequencing

BLAST searches using the rainbow trout CD40L amino acid (aa) sequence identified a 332 bp partial small-spotted catshark CD40L (ScCD40L) cDNA sequence in a 454 RNAseq database generated in-house from spleen mRNA of four shark species including small-spotted catshark (*Scyliorhinus canicula*) and nurse shark (*Ginglymostoma cirratum*) (Crouch *et al*., in preparation). To obtain the complete CD40L cDNA sequence, 3'- and 5'-RACE was performed using the synthesised SMART cDNA (as above) and gene-specific primers (GSP) designed against the partial sequence. All primers used in this work are detailed in Table 1.

No hits were obtained for small-spotted catshark BAFF (ScBAFF) using a similar search strategy so a pair of primers (ScBAFF-F1 and ScBAFF-R1) were designed in the most phylogenetically-conserved region of the molecule and used on spleen cDNA to isolate a 217 bp product. Gene-specific primers were then designed against this product allowing 3'- and 5'-RACE to be attempted. Whilst the 3'-end was completed by RACE using this approach the 5'-RACE reaction initially failed. The complete ScBAFF open reading frame (ORF) was finally obtained by PCR using a primer combination where the forward primer was designed against the spiny dogfish BAFF sequence and the reverse primer against the catshark 3'-RACE product.

The PCR products were cloned as described previously [25]. Plasmid DNA from at least three clones per PCR was extracted using a Qiagen miniprep kit and sequenced by MWG Biotech (Germany). The cDNA sequences of ScCD40L and ScBAFF were validated and submitted to the EMBL/DDJB/GenBank databases under the accession numbers HG326661 (ScCD40L) and HG326662 (ScBAFF).

2.4. Sequence analysis of ScCD40L and ScBAFF

The returned sequences were analysed for similarity with other known sequences using BLAST [27]. The signal peptide was predicted using SignalP v4.0 [28] and the protein family signature was analysed using the PROSITE database of protein families and domains [29]. Transmembrane domains were predicted using TMpred (http://www.ch.embnet.org/software/TMPRED_form.html), N-linked glycosylation sites

were predicted using NetNGlyc 1.0 Server [30] and the furin cleavage site predicted using ProP v1.0 Server [31]. Multiple sequence alignments (MSA) were generated using ClustalΩ (http://www.ebi.ac.uk/Tools/msa/clustalo/) [32].

2.5. Phylogenetic Analysis

Multiple sequence alignments for phylogenetic analyses were generated using MAFFT v.7 [33] via the GUIDANCE webserver [34] using 100 bootstrap guide trees. IQ-TREE was used [35] to determine the best-fit model of amino acid substitution (CD40L+related genes dataset: JTT+I+G4 and BAFF+related genes dataset: JTTDCMut+G4) and subsequently to carry out maximum likelihood phylogenetic analyses specifying 1000 ultrafast bootstrap replicates [35;36]. Bayesian phylogenetic analyses were carried out using PhyloBayes v3.3f [37] under JTT+G4 and CAT+G4 for both datasets to determine the effects of model choice on phylogenetic inference. Two Markov chain Monte Carlo chains were run for each Bayesian analysis and consensus trees were generated following convergence (maxdiff >0.1), with 10% burn-in removed. Phylogenetic trees were visualised in Figtree v1.4.2 (http://tree.bio.ed.ac.uk/software/figtree/).

2.6. *In vivo* expression of ScCD40L and ScBAFF

To determine tissue distribution of ScCD40L and ScBAFF transcript, real-time PCR was performed on selected catshark tissues; spleen, gills, gut, kidney, epigonal and Leydig organ, with muscle included as a non-immune tissue control. Approximately 100 mg of each tissue was chopped into small pieces and immediately homogenised in TRIzol reagent and stored at -80°C until processed for RNA extraction and cDNA synthesis as described above. The comparative expression level of each gene was calculated as arbitrary units where one unit is equal to the average expression level of each gene in muscle, where the lowest expression was observed.

2.7. Isolation of peripheral blood leukocytes from small-spotted catshark

Blood was collected from the caudal vein of catsharks using vacutainers containing lithium heparin, diluted 1:5 in shark-modified cell culture medium (Leibovitz's L-15 medium [38] containing 2% foetal bovine serum (FCS), 100 U/ml penicillin and 100 µg/ml streptomycin (P/S) then adjusted to ~1000 mOsm by the addition of 28 ml of 5M NaCl and 100 ml of 3.5M urea per litre). Peripheral blood leukocytes (PBLs) were isolated from the

diluted blood sample using 38.8% Percoll (Sigma-Aldrich) density gradients diluted in shark-modified medium, and centrifuged at 400 g for 30 min at 8°C. The cells at the interface between the upper aqueous phase and the Percoll solution were collected and washed twice in shark-modified medium. The cells were resuspended and adjusted to a concentration of $2x10^6$ leukocytes/ml with shark-modified medium containing 10% FCS, ready for further treatment.

2.8. Modulation of gene expression in PBLs

Fresh PBLs from four individual fish were prepared at 2×10^6 cells/ml as described above and 2 ml added to the wells of a 6-well plate. The cells were then treated with one of the following stimulants (all from Sigma-Aldrich): PHA at 10µg/ml, PMA at 100 ng/ml, PWM at 100 µg/ml, LPS (serotype 0127 B8) at 25 µg/ml or polyI:C at 50 µg/ml, for 4 , 8 or 24 h at 15°C. The stimulant concentration and stimulatory period were chosen based on splenocyte dose dependency and time-course data sets generated previously by our lab [39;40]. A negative control was set up using shark-modified medium in the place of stimulant. Treatment was terminated by dissolving the cells in TRIzol reagent following their collection by centrifugation at 400 g for 10 min. Total RNA was prepared and transcript levels analysed using real-time PCR quantification as detailed below.

2.9. Quantitative real-time PCR analysis

Real-time PCR was used to determine the abundance of different gene transcripts in tissue samples and isolated PBLs. PCRs were performed in duplicate for each sample, along with a 10-fold serial dilution of a common reference containing an equimolar amount of purified PCR products of each gene amplified from cDNA. The primers employed are given in Table 1; each primer pair was designed to span an intron and was pre-tested to ensure that they did not amplify genomic DNA. Real-time amplification was performed in 96 well plates on a Roche LightCycler 480 real-time PCR system using SYBR green I as described previously [41]. Each reaction contained 4 µl of cDNA template, 14 µl of master mix and 1 µl of each forward and reverse primer.

The relative expression level of the candidate genes in different tissues was expressed as arbitrary units which were calculated from the serial dilution of references run in the same 96-well plate and then normalised against the expression level of the reference gene

elongation factor-1α (EF-1α). To analyse gene expression of stimulated cell cultures, fold changes were calculated as the normalised average expression level of each treatment group divided by that of the corresponding controls at the same time point, where the expression of the control sample was defined as 1. Statistical analysis used the paired-sample *T*-test when comparing expression levels between the control and treated sample, while correlation analysis was performed using the Spearman's nonparametric test within the PASW Statistics 19 software package (SPSS Inc., Chicago, Illinois), as described previously [25]. A ρ value less than 0.05 was considered statistically significant.

3. Results and discussion

3.1. Small-spotted catshark CD40L

The ScCD40L cDNA sequence we cloned is 2457 bp long, containing a 57 bp 5'-UTR, an 867 bp open reading frame (ORF) and a 1533 bp 3'-UTR. The 3'-UTR contains one mRNA instability motif (ATTTA) and three potential polyadenylation signals (AATAAA), the last one being located 13 bp upstream of the poly(A) tail. The predicted ScCD40L protein is 288 amino acids (aa) long with the typical characteristics of a single-pass type II membrane protein having a 24 aa N-terminal cytoplasmic region, a single 24 aa transmembrane domain and a 240 aa C-terminal extracellular region that contains a predicted TNF homology domain (THD), the common structural motif of TNF family ligands. The unglycosylated CD40L monomer has a theoretical molecular mass of 32.8 kDa with three potential N-linked glycosylation sites predicted in the extracellular region.

Using the small-spotted catshark CD40L sequence we were able to retrieve an additional contig from our shark RNAseq database that contained the full-length nurse shark CD40L (GcCD40L). Bayesian and maximum likelihood phylogenetic analysis of vertebrate CD40L and the closely related TNFSF molecules FASL (TNFSF6) and LIGHT (TNFSF14) [42] verified that the cartilaginous fish CD40L molecules are orthologous to bony vertebrate CD40L molecules, and not closely related TNFSF members, with strong support (Fig 1a).

A multiple sequence alignment of selected vertebrate CD40L sequences revealed the pair of cysteines found in the extracellular stalk between the transmembrane region and THD of all species examined so far are also conserved in catshark and nurse shark (Fig 1b). The extracellular region of all tetrapod CD40L's contains three additional Cys, with those in the C and F strands forming an intramolecular disulphide bond that stabilizes the top of the molecule [3]. In teleost fishes these Cys are located in strands E and F and structural modelling of salmon CD40L predicts they are located close enough to form a disulphide bond and thus may have the same stabilising role [43]; these Cys are absent from spotted gar and coelacanth CD40L. Interestingly, only a single additional Cys is found in the extracellular domain of both cartilaginous fish CD40L molecules, positioned in the centre of strand C. When mapped onto the human CD40L crystal structure this lone Cys would be situated on the face of the CD40L monomer involved in trimer formation and would appear

to be buried in this interaction, however the role this Cys plays in homotrimer stabilisation (if any) requires further investigation. In human CD40L the interface between monomers is formed mainly by two tyrosines (Y170 & Y172), two histidines (H224 & H249) and one leucine (L260) [3;44]. Additionally the side chain rings of Y170 stack together in the centre of the homotrimer helping stabilise its structure; this residue is highly conserved across vertebrates, as are Y172 and L260. In contrast both His are poorly conserved across phylogeny suggesting their contribution to trimer stabilisation may be compensated by other residues.

In humans the CD40-binding site consists of a shallow groove formed between two CD40L monomers and is formed mostly from residues in the A-A' and D-E loops; interestingly the A-A' loop in cartilaginous fish CD40 carries a ~14 aa extension when compared to mammalian CD40L. The bony fish also carry an extension of variable length in this region suggesting the structure of the CD40-binding groove may differ considerably between species. Mutational and structural studies performed on human CD40L shows a limited number of residues (specifically K133, E142, K143, Y145, Y146, R200, R203, R207, Q220, E230 and H249; highlighted in black with white lettering in Fig. 1b) contribute to CD40 binding through charge interactions [3;45;46]. These residues are also very poorly conserved in cartilaginous fish CD40L, or indeed any CD40L sequence outside those of mammals (Fig 1b), again suggesting the residues involved in CD40L-CD40 interaction differs between species.

3.2. Small-spotted catshark BAFF

The full-length ScBAFF cDNA sequence was 1103 bp long, with an ORF of 876 bp, encoding a predicted protein of 291 aa, and a 3'-UTR of 218 bp containing one mRNA instability motif and a single poly(A) signal 26 bp upstream of the poly(A) tail. Like ScCD40L the predicted ScBAFF protein is also a typical single-pass type II membrane protein with a 22 aa N-terminal cytoplasmic region, a 23 aa transmembrane domain and a 245 aa C-terminal extracellular region containing a THD domain. Like BAFF in other vertebrates the extracellular region of ScBAFF encodes a furin cleavage site (RNRR) [47] which, if proteolytically cleaved, would release a soluble protein of 177 aa with an unglycosylated molecular mass of 19.9 kDa.

To ensure we had indeed cloned catshark BAFF and not another related TNFSF member we performed a phylogenetic analysis including BAFF molecules from selected vertebrates as well as the closely related TNFSF molecules APRIL and ectodysplasin (EDA) [42]. Both Bayesian and maximum likelihood analyses very strongly support the orthology of ScBAFF, along with the BAFF molecules recently described in spiny dogfish and elephant shark, to each other and the BAFF molecules of other vertebrates (Fig 2a). Interestingly bamboo shark BAFF is not monophyletic with those of the other cartilaginous fishes. In our analysis it falls as an outgroup to the BAFF clade (BPP: 0.99 and 0.97 under CAT+G and JTT+G respectively; bootstrap: 92%), indicating that it had been wrongly assigned in the previous study. This could perhaps be a result of hidden paralogy due to the paucity of sequence data available for cartilaginous fishes. In a previous study it had been noted that spiny dogfish BAFF had an insertion of 28 aa in the 'elbow' region between the A and A' strands, that was lacking in bamboo shark BAFF. A preliminary multiple sequence alignment of the selected vertebrate BAFF molecules showed that catshark BAFF and elephant shark BAFF also have this loop extension but that it is lacking in the bamboo shark molecule [25;26]. The alignment also showed that the bamboo shark sequence was significantly different to the other BAFF molecules in the THD and so the alignment was repeated with the bamboo shark sequence removed (Fig 2b).

As previously observed in spiny dogfish, ScBAFF contains a predicted furin cleavage site (RGRR) between the transmembrane domain and THD suggesting the spotted catshark produces both membrane-bound and soluble forms of BAFF as in mammals; although no cleavage site was found in elephant shark BAFF this could be due to the incomplete nature of the sequence. All three cartilaginous fish BAFF molecules carry the phylogenetically conserved cysteine residues which form the intramolecular disulphide bond between strands E and F, however ScBAFF lacks the Cys usually located at the N-terminal end of the A strand.

As mentioned above ScBAFF, like that of other cartilaginous fish, has a large insertion in the 'elbow' region of the molecule; in human BAFF the elbow contains a short β-hairpin which is located near the D-E loop and together they form the walls of the receptor binding groove in the functional BAFF trimer [48;49]. Molecular models of ScBAFF indicate that the insertion in this region considerably extends the elbow in ScBAFF, however models differ as

to whether the extended anti-parallel β-hairpin protrudes from the surface of the molecule, as with the D-E loop, or if the hairpin folds over so that the extended elbow comes to lie parallel to the others forming the jellyroll. Either way we anticipate the extension in cartilaginous fish BAFF will significantly alter the structure of the receptor binding groove.

In ScBAFF this insertion carries an additional two Cys residues while in elephant shark and dogfish it carries three Cys; we hypothesise the two Cys residues conserved in all three cartilaginous fish BAFFs may form a disulphide bond to help stabilise the extended elbow. The role of the third Cys in elephant shark and spiny dogfish is, as yet, undetermined but potentially could pair with the free, solvent exposed Cys in the A strand [2] that is also missing in catshark BAFF.

Residues shown by structural studies to be integral in the formation of human BAFF trimers [2;16] (specifically Q144, Y192, F194, Y196, Q234, Y246, F278 & L285; shown in dark grey in Fig 2b) are highly conserved throughout vertebrate phylogeny, as are the three residues (Q234, N235 & N243; shown in bold on Fig 2b) that form the Mg^{2+}-binding site that helps stabilise the narrow end of the trimer [48]. Both catshark and elephant shark BAFF molecules also carry a pair of cysteines that map to the tip of the E-F loop on the human BAFF structure and which may help further stabilize this region by forming either inter- or intraloop disulphide bonds.

As detailed above, at neutral or basic pH mammalian BAFF associates into a 60-mer virus-like structure [16]. The ability to form these multimers is dependent upon interactions between the extended D-E loops of adjacent BAFF trimers, is pH-dependent and requires a particular His residue (H218; blue in Fig 2b) within the D-E loop; mutation of this residue to Ala abolished multimer formation however the mutant BAFF protein retained biological activity [50]. This His is absent from all of the cartilaginous fish BAFF molecules, as well as those from bony fishes (with the exception of spotted gar); indeed, from current sequence data it seems this His is only present in amniotes and suggests that cartilaginous fish BAFF may not be able to form stable multimers.

ScBAFF has two predicted N-linked glycosylation sites, including one at the beginning of the F strand that is conserved in the other cartilaginous fishes and in tetrapods (but not bony fishes). Structural studies have shown this site is indeed glycosylated in human BAFF

and makes contact with a Tyr at the beginning of the D strand (Y206) and an Arg within the E strand (R231) [2]; the latter is conserved in all cartilaginous fishes while the Tyr is replaced by the structurally similar Phe.

Previous structural studies have identified a number of residues in human BAFF that are involved in its binding to BAFF-R, BCMA and TACI [51;52;53] (highlighted in black with white lettering in Fig 2b). The residues from β-strands D and E, as well as the residues between the G and H strands, which form the base and walls of the receptor binding site are reasonably well conserved across phylogeny.

3.3. Tissue distribution of ScCD40L and ScBAFF

Transcript levels of these two genes were examined in seven tissues from four healthy small-spotted catsharks (Fig 3). Unfortunately thymus tissue was not available for examination in this study. Real-time PCR analysis revealed that both genes showed detectable transcript levels in all of the tissues tested, with muscle expressing the lowest levels of each. ScCD40L transcript was highest in the gut and spleen followed by gill, Leydig organ, kidney and epigonal, with constitutive expression levels being up to 8,000 fold greater in these immune organs than in muscle. Further, the levels of ScCD40L transcript correlated with that of TCRα transcript but not with that of the B cell marker CD79α (Table 2); when combined with our previous work [54] this suggests that, as in mammals, catshark CD40L is expressed on T cells.

Similarly, ScBAFF transcript levels were 100-2,500 fold higher in immune organs than in muscle, being found at the highest level in spleen (fitting with this being the main secondary immune organ in sharks), followed by gill, epigonal, gut, kidney and Leydig organ (Fig 3).

3.4. Modulation of the expression of ScCD40L and BAFF in PBLs

To assess the effect of various mitogens and PAMPs upon CD40L and BAFF expression PBLs were harvested from four healthy catsharks and transcript levels of the two genes studied following stimulation with polyI:C, LPS, PHA, PMA and PWM for 4, 8 or 24 h (Fig 4). In this study, ScCD40L expression was upregulated ~15-fold by PHA at 4 h and ~7.5-fold at 8 h. ScCD40L expression was also significantly upregulated by both PMA and PWM at

24 h (~11-fold and 9-fold respectively) however polyI:C and LPS had no effect upon ScCD40L expression.

In contrast, ScBAFF expression could not be induced with PHA, PMA or polyI:C (Fig. 4). A small but significant up-regulation (~2 to 4-fold) in the expression of ScBAFF was observed after 8 h and 24 h with PWM or after 24 h with LPS (~2-fold) correlating with data previously obtained in spiny dogfish [25]. In mammals LPS has long been known to be a potent B cell mitogen [55;56] however this study and our previous work [25; Dooley and Flajnik, unpublished data], suggests cartilaginous fishes are relatively LPS unresponsive; indeed TLR4, the main receptor for LPS in mammals appears to have been lost in at least some cartilaginous fish species [24 ; Dooley *et al*, unpublished data].

4. Conclusions

TNFSF members play critical roles in many aspects of immune organisation and functioning. By characterising these molecules in cartilaginous fishes, the most ancient group with a canonical vertebrate adaptive immune system, we hope to better understand TNFSF evolution. In this work we characterised the TNFSF members CD40L and BAFF in the small-spotted catshark; while both molecules had the traditional TNFSF features previously described in their vertebrate orthologues both cartilaginous fish molecules carried an extension in their A-A' loop (termed the 'elbow' in BAFF) when compared to those of other vertebrates. In human CD40L and BAFF this loop forms an integral part of the receptor binding groove and so changes to this region could significantly alter its structure. However as TNFSF receptors and ligands generally co-evolve it is highly likely that cartilaginous fish CD40 will have compensatory changes in its structure to ensure interaction of the two still occurs. As three potential CD40 molecules were identified by Venkatesh and colleagues [24] during their survey of the elephant shark genome, and we have recently found a partial sequence for catshark CD40 (data not shown) there is the possibility of performing functional studies to examine CD40-CD40L binding/functioning in cartilaginous fishes at some point in the future.

Although BAFF has previously been cloned from two different species of cartilaginous fish, bamboo shark and spiny dogfish, notable differences were observed between the two molecules in terms of structure and tissue expression. Through the

addition of catshark and elephant shark BAFF the combined data suggests that the bamboo shark molecule is almost certainly not BAFF, and likely represents an ancient gnathostome BAFF paralogue. Similarly, although APRIL has not yet been cloned from a cartilaginous fish (and could not be found in the elephant shark genome sequence), the bamboo shark molecule is highly unlikely to be APRIL, given the tree topology in Fig 2a. Another molecule, BALM (for BAFF-APRIL-like molecule), with similarity to both BAFF and APRIL was recently found in bony fishes [42] and comparison of the TNFSF phylogeny generated in that study combined with the analyses performed here suggests that the bamboo molecule is most plausibly the cartilaginous fish orthologue of BALM, if that of any previously identified TNFSF member. The acquisition of more TNFSF sequences from cartilaginous fishes will improve our understanding of the evolution of this multi-gene family and should help resolve such questions of orthology.

Although LPS and polyI:C are both potent immune stimulants in mammals neither had a significant impact upon the transcript levels of ScCD40L or ScBAFF in this study (Fig 4). Interestingly, those immunostimulants that did elicit a response did so with very different response kinetics; for example, following treatment with PHA transcript levels of ScCD40L increased to a maximum around 4 h then decreased back to pre-stimulation levels by 24 h. However, following treatment with PMA or PWM transcript levels of the same gene increased slowly, with maximum observed expression at 24 h. Although the response for ScBAFF was modest compared to ScCD40L, the kinetics of expression were similar following stimulation with PHA (early) and PWM (late). It seems likely that these differences in transcription kinetics reflect variation in the pattern-recognition receptors (PRRs) engaged by each immunostimulant and the signalling pathways subsequently triggered. The recent survey of the elephant shark genome showed that cartilaginous fishes possess a diverse repertoire of PRRs including many mammalian-like TLRs [24]; TLR4 was notably absent, perhaps explaining the lack of LPS responsiveness observed in this and other studies [24;25; Dooley and Flajnik, unpublished data]. However, excepting a single study profiling the tissue expression of TLR2 in bamboo shark [57] very little is known about the functioning of TLRs in cartilaginous fishes. Until a robust functional study is undertaken we cannot simply assume that the expression patterns and ligand specificities of cartilaginous fish PRRs will be identical to their mammalian counterparts.

Figure legends

Figure 1. (a) Midpoint rooted Bayesian consensus tree showing the relationship of catshark CD40L (shaded in grey), as generated under the CAT+G4 model in PhyloBayes [37] (support values displayed in format: BPP: CAT+G4/BPP: JTT+G4/bootstrap: JTT+I+G4) with related TNFSF family members from other species. The accession numbers of the sequences used for the phylogenetic analysis are as follows: human CD40L gi|231718, FASL gi|1345957, LIGHT gi|49456663; Xenopus CD40L gi|301606052, FASL gi|209969497, LIGHT gi|512876905; Chicken CD40L gi|38503419, FASL gi|61656613; Anole CD40L gi|637358319, FASL gi|637338609, LIGHT gi|637263772; Coelacanth CD40L ENSLACP00000017831, FASL gi|556985919, LIGHT gi|556972368 or gi|556972365; Spotted gar CD40L gi|573890595, FASL gi|573895222, LIGHT gi|573887909 or gi|573887911; Zebrafish CD40L gi|221307465, FASL gi|111607490, LIGHT gi|393191965; Salmon CD40L gi|221221084; Elephant shark CD40L SINCAMP00000023076, FASL SINCAMP00000024563. **(b)** Multiple sequence alignment of catshark CD40L with other vertebrate CD40L molecules. Cysteines are highlighted in light grey and predicted N-linked glycosylation sites are boxed. Sites shown to be involved in CD40L-CD40 binding in human are shown in black with white lettering while residues important in trimer formation are shown in dark grey. Individual β-strands (A-H) of ScCD40L are indicated by arrows above the alignment; the insertion in the A-A' loop of cartilaginous fish CD40L is highlighted in red and the shark-specific unpaired Cys in yellow. Alignments were generated with ClustalΩ [32] and the accession numbers of the sequences used are as above.

Figure 2. (a) Midpoint rooted Bayesian consensus tree showing the relationship of catshark BAFF (shaded in grey), as generated under the JTT+G4 model in PhyloBayes [37] (support values displayed in format: BPP: JTT+G4/BPP: CAT+G4/bootstrap: JTTDCmut+G4), with related TNFSF family members from other species. The bamboo shark protein previously identified as BAFF by Ren and colleagues [26] is circled. The accession numbers of the sequences used for the phylogenetic analysis are as follows: human BAFF gi|13124573, APRIL gi|13124605, EDA gi|6166135; Xenopus BAFF gi|510788204, APRIL gi|525506957, EDA gi|301610844; Chicken BAFF gi|24432186, EDA gi|513181553; Anole BAFF gi|637251511, APRIL gi|637362069; Coelacanth BAFF gi|556980947, EDA gi|556981351;

Spotted gar BAFF gi|573903189, APRIL gi|573878509, EDA gi|573890256; Zebrafish BAFF gi|165972407, APRIL gi|270309104, EDA gi|169234872; Trout BAFF gi|85822187; Bamboo shark BAFF* gi|326366338; Spiny dogfish BAFF gi|527482306, Elephant shark BAFF SINCAMP00000022579, EDA gi|632936255. **(b)** Multiple sequence alignment of catshark BAFF with other vertebrate BAFF molecules. The transmembrane domain (TMD) is underlined and potential furin cleavage sites are highlighted in light grey and double underlined. Cysteines are highlighted in light grey and predicted N-linked glycosylation sites are boxed. Sites shown to be involved in receptor binding in human BAFF are shown in black with white lettering while residues involved in trimer formation are shown in dark grey. The residues that form the metal binding site and play an important role in stabilising the trimer in human are shown in bold. Individual β-strands (A-H) are indicated by arrows above the alignment; the 28 aa insertion found in the elbow region of cartilaginous fish BAFF is highlighted in red while the long D-E loop characteristic of BAFF is boxed. H218, which facilitates the formation of BAFF multimers in mammals, is highlighted in blue. Alignments were generated with ClustalΩ [32] and the accession numbers of the sequences used are as above.

Figure 3. Constitutive expression levels of catshark CD40L, BAFF and TCRα *in vivo*. The relative expression levels of the three genes in eight small-spotted catshark tissues are expressed as arbitrary units normalised against the expression level of the reference gene EF-1α. To allow comparison the average expression level of each gene in muscle, where the expression level was lowest, was defined as 1. The results are presented as the mean +SEM for four animals.

Figure 4. Changes in expression of CD40L and BAFF in catshark PBLs treated with various stimulants. The PBLs from small-spotted catshark were incubated with polyI:C, LPS, PHA, PMA, or PWM at 15°C for 4 h, 8 h and 24 h. The expression levels of these two genes were normalised against that of the reference gene EF-1α then divided by their respective control samples, which were defined as 1 at the same time point. All results are presented as averages + standard error of cells from four animals, and values are significantly different to

the unstimulated control at the same time point when marked with asterisks (*P <0.05; **P <0.01; ***P <0.001).

Acknowledgements

This work was supported financially by a BBSRC Industrial CASE Studentship with Pfizer to RL.

References

[1] Locksley RM, Killeen N, Lenardo MJ. The TNF and TNF receptor superfamilies: integrating mammalian biology. *Cell* 2001; 104(4):487-501.

[2] Karpusas M, Cachero TG, Qian F, Boriack-Sjodin A, Mullen C, Strauch K et al. Crystal structure of extracellular human BAFF, a TNF family member that stimulates B lymphocytes. *J Mol Biol* 2002; 315(5):1145-1154.

[3] Karpusas M, Hsu YM, Wang JH, Thompson J, Lederman S, Chess L et al. 2 A crystal structure of an extracellular fragment of human CD40 ligand. *Structure* 1995; 3(12):1426.

[4] Eck MJ, Sprang SR. The structure of tumor necrosis factor-alpha at 2.6Å resolution. Implications for receptor binding. *J Biol Chem* 1989; 264(29):17595-17605.

[5] Eck MJ, Ultsch M, Rinderknecht E, de Vos AM, Sprang SR. The structure of human lymphotoxin (tumor necrosis factor-beta) at 1.9Å resolution. *J Biol Chem* 1992; 267(4):2119-2122.

[6] van Kooten C, Banchereau J. CD40-CD40 ligand. *J Leukoc Biol* 2000; 67(1):2-17.

[7] Leveille,C., Bouillon,M., Guo,W., Bolduc,J., Sharif-Askari,E., El-Fakhry,Y., Reyes-Moreno,C., Lapointe,R., Merhi,Y., Wilkins,J.A., Mourad,W. CD40 ligand binds to alpha5beta1 integrin and triggers cell signaling. *J Biol Chem* 2007; 282(8):5143-5151.

[8] Andre,P., Prasad,K.S., Denis,C.V., He,M., Papalia,J.M., Hynes,R.O., Phillips,D.R., Wagner,D.D. CD40L stabilizes arterial thrombi by a beta3 integrin-dependent mechanism. *Nat Med* 2002; 8(3):247-252.

[9] Zirlik,A., Maier,C., Gerdes,N., MacFarlane,L., Soosairajah,J., Bavendiek,U., Ahrens,I., Ernst,S., Bassler,N., Missiou,A., Patko,Z., Aikawa,M., Schonbeck,U., Bode,C., Libby,P., Peter,K. CD40 ligand mediates inflammation independently of CD40 by interaction with Mac-1. *Circulation* 2007; 115(12):1571-1580.

[10] Kawabe,T., Naka,T., Yoshida,K., Tanaka,T., Fujiwara,H., Suematsu,S., Yoshida,N., Kishimoto,T., Kikutani,H. The immune responses in CD40-deficient mice: impaired immunoglobulin class switching and germinal center formation. *Immunity* 1994; 1(3):167-178.

[11] Xu,J., Foy,T.M., Laman,J.D., Elliott,E.A., Dunn,J.J., Waldschmidt,T.J., Elsemore,J., Noelle,R.J., Flavell,R.A. Mice deficient for the CD40 ligand. *Immunity* 1994; 1(5):423-431.

[12] Castigli,E., Alt,F.W., Davidson,L., Bottaro,A., Mizoguchi,E., Bhan,A.K., Geha,R.S. CD40-deficient mice generated by recombination-activating gene-2-deficient blastocyst complementation. *Proc Natl Acad Sci U S A* 1994; 91(25):12135-12139.

[13] Grewal IS, Flavell RA. The role of CD40 ligand in costimulation and T-cell activation. *Immunol Rev* 1996; 153:85-106.

[14] Nardelli,B., Belvedere,O., Roschke,V., Moore,P.A., Olsen,H.S., Migone,T.S., Sosnovtseva,S., Carrell,J.A., Feng,P., Giri,J.G., Hilbert,D.M. Synthesis and release of B-lymphocyte stimulator from myeloid cells. *Blood* 2001; 97(1):198-204.

[15] Huard,B., Arlettaz,L., Ambrose,C., Kindler,V., Mauri,D., Roosnek,E., Tschopp,J., Schneider,P., French,L.E. BAFF production by antigen-presenting cells provides T cell co-stimulation. *Int Immunol* 2004; 16(3):467-475.

[16] Liu Y, Xu L, Opalka N, Kappler J, Shu HB, Zhang G. Crystal structure of sTALL-1 reveals a virus-like assembly of TNF family ligands. *Cell* 2002; 108(3):383-394.

[17] Bossen C, Schneider P. BAFF, APRIL and their receptors: structure, function and signaling. *Semin Immunol* 2006; 18(5):263-275.

[18] Bossen,C., Ingold,K., Tardivel,A., Bodmer,J.L., Gaide,O., Hertig,S., Ambrose,C., Tschopp,J., Schneider,P. Interactions of tumor necrosis factor (TNF) and TNF receptor family members in the mouse and human. *J Biol Chem* 2006; 281(20):13964-13971.

[19] Ingold,K., Zumsteg,A., Tardivel,A., Huard,B., Steiner,Q.G., Cachero,T.G., Qiang,F., Gorelik,L., Kalled,S.L., Acha-Orbea,H., Rennert,P.D., Tschopp,J., Schneider,P. Identification of proteoglycans as the APRIL-specific binding partners. *J Exp Med* 2005; 201(9):1375-1383.

[20] Treml JF, Hao Y, Stadanlick JE, Cancro MP. The BLyS family: toward a molecular understanding of B cell homeostasis. *Cell Biochem Biophys* 2009; 53(1):1-16.

[21] Flajnik MF, Kasahara M. Origin and evolution of the adaptive immune system: genetic events and selective pressures. *Nat Rev Genet* 2010; 11(1):47-59.

[22] Crouch,K., Smith,L.E., Williams,R., Cao,W., Lee,M., Jensen,A., Dooley,H. Humoral immune response of the small-spotted catshark, *Scyliorhinus canicula*. *Fish Shellfish Immunol* 2013; 34(5):1158-1169.

[23] Dooley H, Flajnik MF. Shark immunity bites back: affinity maturation and memory response in the nurse shark, *Ginglymostoma cirratum*. *Eur J Immunol* 2005.

[24] Venkatesh,B., Lee,A.P., Ravi,V., Maurya,A.K., Lian,M.M., Swann,J.B., Ohta,Y., Flajnik,M.F., Sutoh,Y., Kasahara,M., Hoon,S., Gangu,V., Roy,S.W., Irimia,M., Korzh,V., Kondrychyn,I., Lim,Z.W., Tay,B.H., Tohari,S., Kong,K.W., Ho,S., Lorente-Galdos,B., Quilez,J., Marques-Bonet,T., Raney,B.J., Ingham,P.W., Tay,A., Hillier,L.W., Minx,P., Boehm,T., Wilson,R.K., Brenner,S., Warren,W.C. Elephant shark genome provides unique insights into gnathostome evolution. *Nature* 2014; 505(7482):174-179.

[25] Li R, Dooley H, Wang T, Secombes CJ, Bird S. Characterisation and expression analysis of B-cell activating factor (BAFF) in spiny dogfish (*Squalus acanthias*): Cartilaginous fish BAFF has a unique extra exon that may impact receptor binding. *Dev Comp Immunol* 2011.

[26] Ren W, Pang S, You F, Zhou L, Zhang S. The first BAFF gene cloned from the cartilaginous fish. *Fish Shellfish Immunol* 2011; 31(6):1088-1096.

[27] Altschul SF, Gish W, Miller W, Myers EW, Lipman DJ. Basic local alignment search tool. *J Mol Biol* 1990; 215(3):403-410.

[28] Petersen TN, Brunak S, von HG, Nielsen H. SignalP 4.0: discriminating signal peptides from transmembrane regions. *Nat Methods* 2011; 8(10):785-786.

[29] Sigrist,C.J., Cerutti,L., de,C.E., Langendijk-Genevaux,P.S., Bulliard,V., Bairoch,A., Hulo,N. PROSITE, a protein domain database for functional characterization and annotation. *Nucleic Acids Res* 2010; 38(Database issue):D161-D166.

[30] Salim A, Bano A, Zaidi ZH. Prediction of possible sites for posttranslational modifications in human gamma crystallins: effect of glycation on the structure of human gamma-B-crystallin as analyzed by molecular modeling. *Proteins* 2003; 53(2):162-173.

[31] Duckert P, Brunak S, Blom N. Prediction of proprotein convertase cleavage sites. *Protein Eng Des Sel* 2004; 17(1):107-112.

[32] Sievers,F., Wilm,A., Dineen,D., Gibson,T.J., Karplus,K., Li,W., Lopez,R., McWilliam,H., Remmert,M., Soding,J., Thompson,J.D., Higgins,D.G. Fast, scalable generation of high-quality protein multiple sequence alignments using Clustal Omega. *Mol Syst Biol* 2011; 7:539.

[33] Katoh K, Standley DM. MAFFT multiple sequence alignment software version 7: improvements in performance and usability. *Mol Biol Evol* 2013; 30(4):772-780.

[34] Penn O, Privman E, Ashkenazy H, Landan G, Graur D, Pupko T. GUIDANCE: a web server for assessing alignment confidence scores. *Nucleic Acids Res* 2010; 38(Web Server issue):W23-W28.

[35] Nguyen LT, Schmidt HA, von Haeseler A, Minh BQ. IQ-TREE: a fast and effective stochastic algorithm for estimating maximum-likelihood phylogenies. *Mol Biol Evol* 2015; 32(1):268-274.

[36] Minh BQ, Nguyen MA, von Haeseler A. Ultrafast approximation for phylogenetic bootstrap. *Mol Biol Evol* 2013; 30(5):1188-1195.

[37] Lartillot N, Lepage T, Blanquart S. PhyloBayes 3: a Bayesian software package for phylogenetic reconstruction and molecular dating. *Bioinformatics* 2009; 25(17):2286-2288.

[38] Leibovitz A. THE GROWTH AND MAINTENANCE OF TISSUE-CELL CULTURES IN FREE GAS EXCHANGE WITH THE ATMOSPHERE. *Am J Hyg* 1963; 78:173-180.

[39] Bird S, Wang T, Zou J, Cunningham C, Secombes CJ. The first cytokine sequence within cartilaginous fish: IL-1 beta in the small spotted catshark (*Scyliorhinus canicula*). *J Immunol* 2002; 168(7):3329-3340.

[40] Wang T, Monte MM, Huang W, Boudinot P, Martin SA, Secombes CJ. Identification of two FoxP3 genes in rainbow trout (*Oncorhynchus mykiss*) with differential induction patterns. *Mol Immunol* 2010; 47(16):2563-2574.

[41] Wang,T., Diaz-Rosales,P., Costa,M.M., Campbell,S., Snow,M., Collet,B., Martin,S.A., Secombes,C.J. Functional characterization of a nonmammalian IL-21: rainbow trout *Oncorhynchus mykiss* IL-21 upregulates the expression of the Th cell signature cytokines IFN-gamma, IL-10, and IL-22. *J Immunol* 2011; 186(2):708-721.

[42] Glenney GW, Wiens GD. Early diversification of the TNF superfamily in teleosts: genomic characterization and expression analysis. *J Immunol* 2007; 178(12):7955-7973.

[43] Lagos LX, Iliev DB, Helland R, Rosemblatt M, Jorgensen JB. CD40L - a costimulatory molecule involved in the maturation of antigen presenting cells in Atlantic salmon (*Salmo salar*). *Dev Comp Immunol* 2012; 38(3):416-430.

[44] Peitsch MC, Jongeneel CV. A 3-D model for the CD40 ligand predicts that it is a compact trimer similar to the tumor necrosis factors. *Int Immunol* 1993; 5(2):233-238.

[45] Singh,J., Garber,E., Van,V.H., Karpusas,M., Hsu,Y.M., Zheng,Z., Naismith,J.H., Thomas,D. The role of polar interactions in the molecular recognition of CD40L with its receptor CD40. *Protein Sci* 1998; 7(5):1124-1135.

[46] An,H.J., Kim,Y.J., Song,D.H., Park,B.S., Kim,H.M., Lee,J.D., Paik,S.G., Lee,J.O., Lee,H. Crystallographic and mutational analysis of the CD40-CD154 complex and its implications for receptor activation. *J Biol Chem* 2011; 286(13):11226-11235.

[47] Schneider,P., Mackay,F., Steiner,V., Hofmann,K., Bodmer,J.L., Holler,N., Ambrose,C., Lawton,P., Bixler,S., Acha-Orbea,H., Valmori,D., Romero,P., Werner-Favre,C.,

Zubler,R.H., Browning,J.L., Tschopp,J. BAFF, a novel ligand of the tumor necrosis factor family, stimulates B cell growth. *J Exp Med* 1999; 189(11):1747-1756.

[48] Oren,D.A., Li,Y., Volovik,Y., Morris,T.S., Dharia,C., Das,K., Galperina,O., Gentz,R., Arnold,E. Structural basis of BLyS receptor recognition. *Nat Struct Biol* 2002; 9(4):288-292.

[49] Kim,H.M., Yu,K.S., Lee,M.E., Shin,D.R., Kim,Y.S., Paik,S.G., Yoo,O.J., Lee,H., Lee,J.O. Crystal structure of the BAFF-BAFF-R complex and its implications for receptor activation. *Nat Struct Biol* 2003; 10(5):342-348.

[50] Cachero,T.G., Schwartz,I.M., Qian,F., Day,E.S., Bossen,C., Ingold,K., Tardivel,A., Krushinskie,D., Eldredge,J., Silvian,L., Lugovskoy,A., Farrington,G.K., Strauch,K., Schneider,P., Whitty,A. Formation of virus-like clusters is an intrinsic property of the tumor necrosis factor family member BAFF (B cell activating factor). *Biochemistry* 2006; 45(7):2006-2013.

[51] Liu,Y., Hong,X., Kappler,J., Jiang,L., Zhang,R., Xu,L., Pan,C.H., Martin,W.E., Murphy,R.C. Ligand-receptor binding revealed by the TNF family member TALL-1. *Nature* 2003; 423(6935):49-56.

[52] Gordon,N.C., Pan,B., Hymowitz,S.G., Yin,J., Kelley,R.F., Cochran,A.G., Yan,M., Dixit,V.M., Fairbrother,W.J., Starovasnik,M.A. BAFF/BLyS receptor 3 comprises a minimal TNF receptor-like module that encodes a highly focused ligand-binding site. *Biochemistry* 2003; 42(20):5977-5983.

[53] Wang,R., Wang,R., Ma,N., Guo,Y., Xiao,H., Chen,G., Han,G., Hou,C., Shen,B., Feng,J., Li,Y. Identify the key amino acid of BAFF binding with TACI. *Cell Immunol* 2013; 284(1-2):84-90.

[54] Li R, Wang T, Bird S, Zou J, Dooley H, Secombes CJ. B cell receptor accessory molecule CD79alpha: characterisation and expression analysis in a cartilaginous fish, the spiny dogfish (*Squalus acanthias*). *Fish Shellfish Immunol* 2013; 34(6):1404-1415.

[55] Andersson J, Sjoberg O, Moller G. Induction of immunoglobulin and antibody synthesis in vitro by lipopolysaccharides. *Eur J Immunol* 1972; 2(4):349-353.

[56] Andersson J, Moller G, Sjoberg O. Selective induction of DNA synthesis in T and B lymphocytes. *Cell Immunol* 1972; 4(4):381-393.

[57] Anandhakumar,C., Lavanya,V., Pradheepa,G., Tirumurugaan,K.G., Raj,G.D., Raja,A., Pazhanivel,N., Balachandran,C. Expression profile of toll-like receptor 2 mRNA in selected tissues of shark (*Chiloscyllium sp.*). *Fish Shellfish Immunol* 2012; 33(5):1174-1182.

Table 1. Primers used for the cloning and expression analysis of catshark CD40L and BAFF

Primer	Sequence (5'-3')	n	Application
ScCD40L-F1	CCAGCCCGGATTTTACTATGTGTATTG	27	cloning (3'-RACE)
ScCD40L-F2	GTTTCCGACTAACCAACAACGTCAC	25	cloning (3'-RACE)
ScCD40L-R1	CTCCTGTTTTTAACTCAAACACTCCTCC	28	cloning (5'-RACE)
ScCD40L-R2	TGTCGACTGGTGTTTTGGATGC	22	cloning (5'-RACE)
ScBAFF-F1	ACAACTGTCCCATGGATTCTGAG	23	cloning (partial coding region)
ScBAFF-R1	TGTTTTGGATGCACCGAAATAGG	23	cloning (partial coding region)
ScBAFF-F2	CGAGGCTGGCTTCTTTCTGG	20	cloning (3'-RACE)
ScBAFF-F3	TCAAGAGAATAAAGGCCAGCAGTG	24	cloning (3'-RACE)
ScBAFF-F	GAATTTGGGATGAAGATGAGAATG	24	cloning (coding region)
ScBAFF-R	CTCGACTGCCTTAGCCATCACAG	23	cloning (coding region)
ScCD40L-RTF	TCAATGAAACTTGACAAGGTTCAGG	25	real-time PCR
ScCD40L-RTR	GATGGTTACCTATCTGTTTTTCTTGCGT	28	real-time PCR
ScBAFF-RTF	CTTTCTGGTGTACAGTCAGGTGTGG	25	real-time PCR
BAFF-RTR	CAAGTTTTGCAATGCCAGCAG	21	real-time PCR
ScEF1α-RTF	CGTCTTCCTTTATTGCACAGGTTATTATC	29	real-time PCR
ScEF1α-RTR	GGACAGCGAAACGACCAAGAG	21	real-time PCR
ScTCRα-RTF	TGCCTGGTGACGGATTATTTCC	22	real-time PCR
ScTCRα-RTR	GGAAAGGGTGTTCAAGTGTTCGAC	24	real-time PCR

Table 2. Expression of ScCD40L correlates with that of ScTCRα but not ScCD79α

		CD40L	TCRα	CD79α
CD40L	Correlation Coefficient(R)	1	0.821**	0.071
	Significance (*p*)		0	0.857
	N	28	28	28

** Correlation is significant at the 0.01 level (2-tailed)

a)

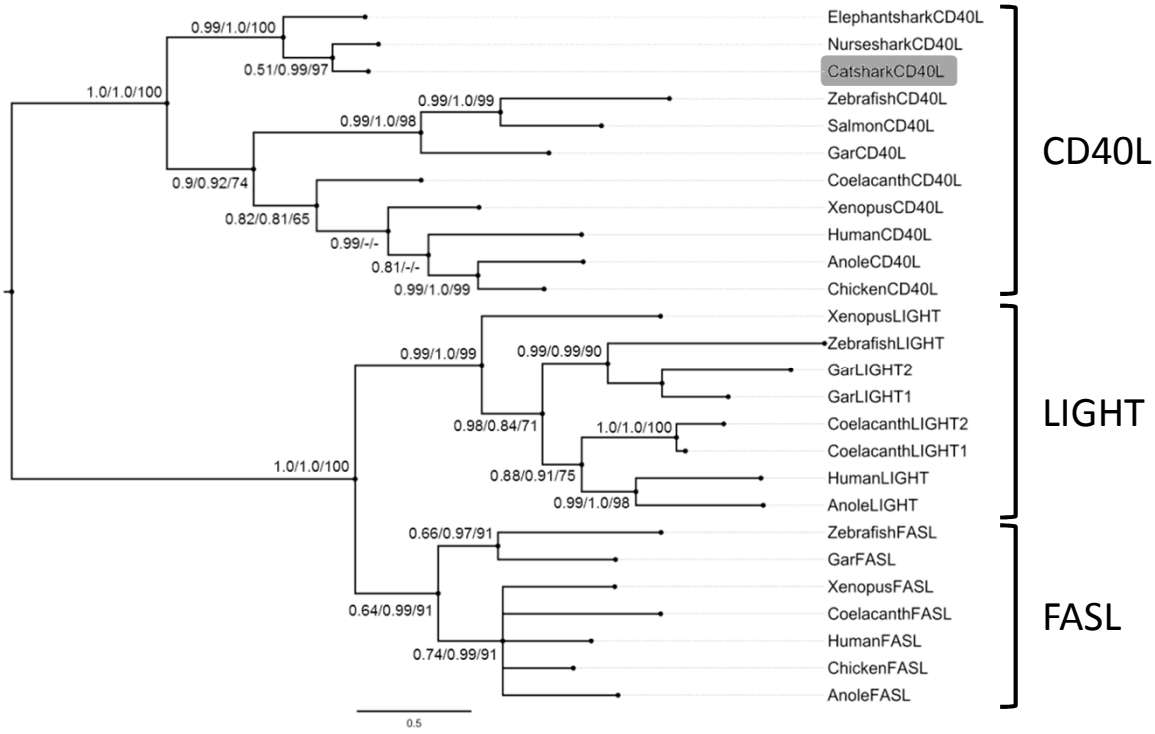
0.99/1.0/100
0.51/0.99/97
1.0/1.0/100
0.99/1.0/99
0.99/1.0/98
0.9/0.92/74
0.82/0.81/65
0.99/-/-
0.81/-/-
0.99/1.0/99
0.99/1.0/99
0.99/0.99/90
0.98/0.84/71
1.0/1.0/100
1.0/1.0/100
0.88/0.91/75
0.99/1.0/98
0.66/0.97/91
0.64/0.99/91
0.74/0.99/91
0.5
ElephantsharkCD40L
NursesharkCD40L
CatsharkCD40L
ZebrafishCD40L
SalmonCD40L
GarCD40L
CoelacanthCD40L
XenopusCD40L
HumanCD40L
AnoleCD40L
ChickenCD40L
XenopusLIGHT
ZebrafishLIGHT
GarLIGHT2
GarLIGHT1
CoelacanthLIGHT2
CoelacanthLIGHT1
HumanLIGHT
AnoleLIGHT
ZebrafishFASL
GarFASL
XenopusFASL
CoelacanthFASL
HumanFASL
ChickenFASL
AnoleFASL
CD40L
LIGHT
FASL

b)

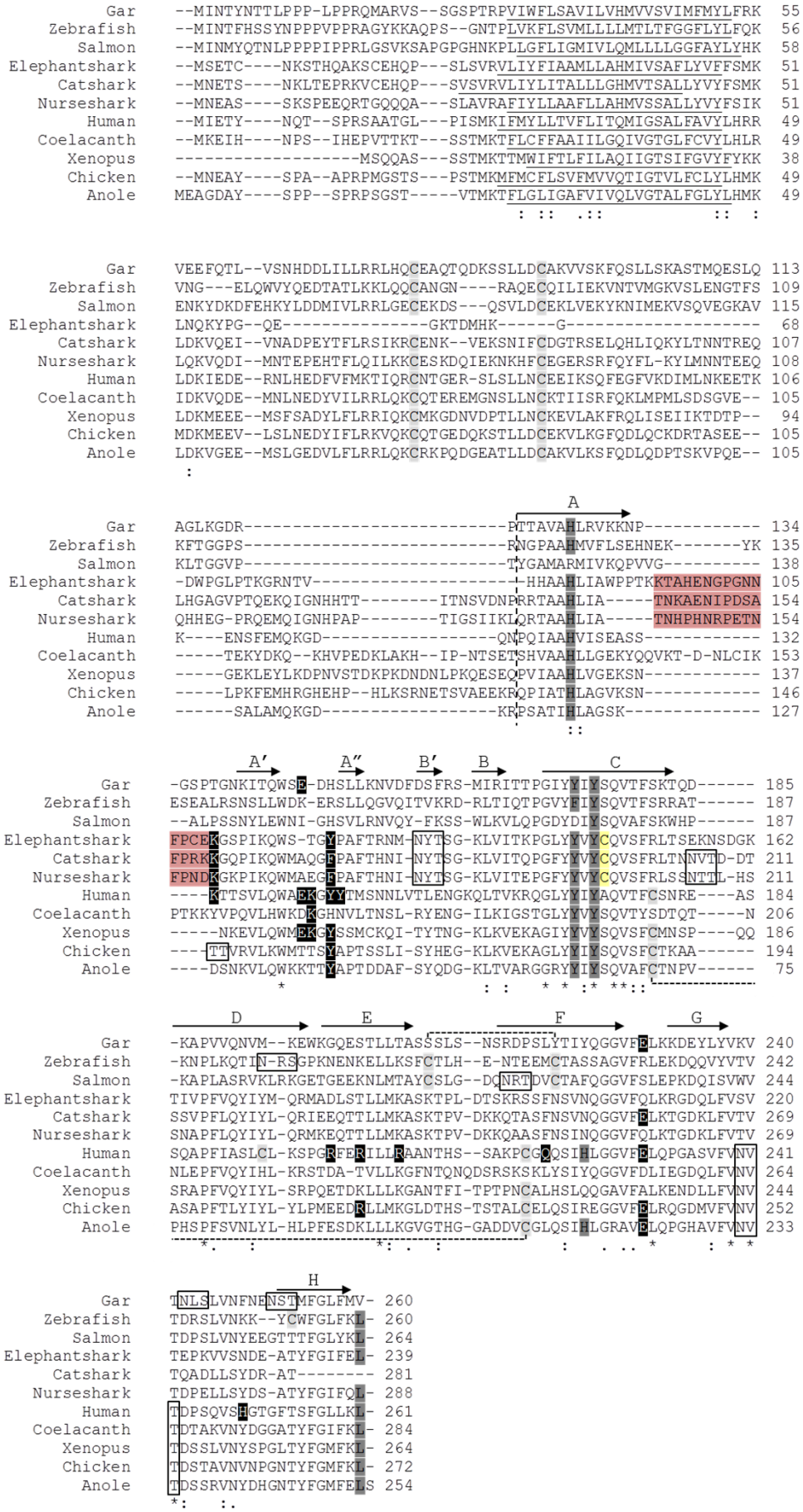

a)

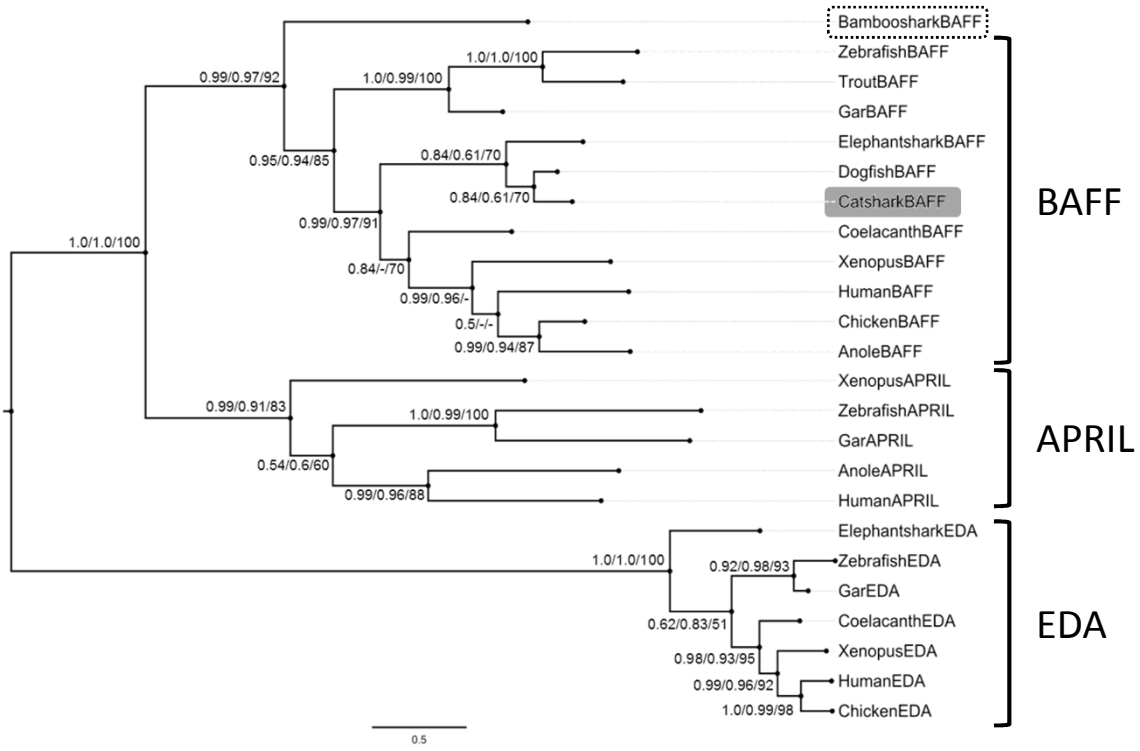
BambooSharkBAFF
ZebrafishBAFF
TroutBAFF
GarBAFF
ElephantsharkBAFF
DogfishBAFF
CatsharkBAFF
CoelacanthBAFF
XenopusBAFF
HumanBAFF
ChickenBAFF
AnoleBAFF
XenopusAPRIL
ZebrafishAPRIL
GarAPRIL
AnoleAPRIL
HumanAPRIL
ElephantsharkEDA
ZebrafishEDA
GarEDA
CoelacanthEDA
XenopusEDA
HumanEDA
ChickenEDA
BAFF
APRIL
EDA
1.0/1.0/100
0.99/0.97/92
1.0/0.99/100
0.95/0.94/85
0.84/0.61/70
0.84/0.61/70
0.99/0.97/91
1.0/1.0/100
0.84/-/70
0.99/0.96/-
0.5/-/-
0.99/0.94/87
0.99/0.91/83
1.0/0.99/100
0.54/0.6/60
0.99/0.96/88
1.0/1.0/100
0.92/0.98/93
0.62/0.83/51
0.98/0.93/95
0.99/0.96/92
1.0/0.99/98
0.5

b)

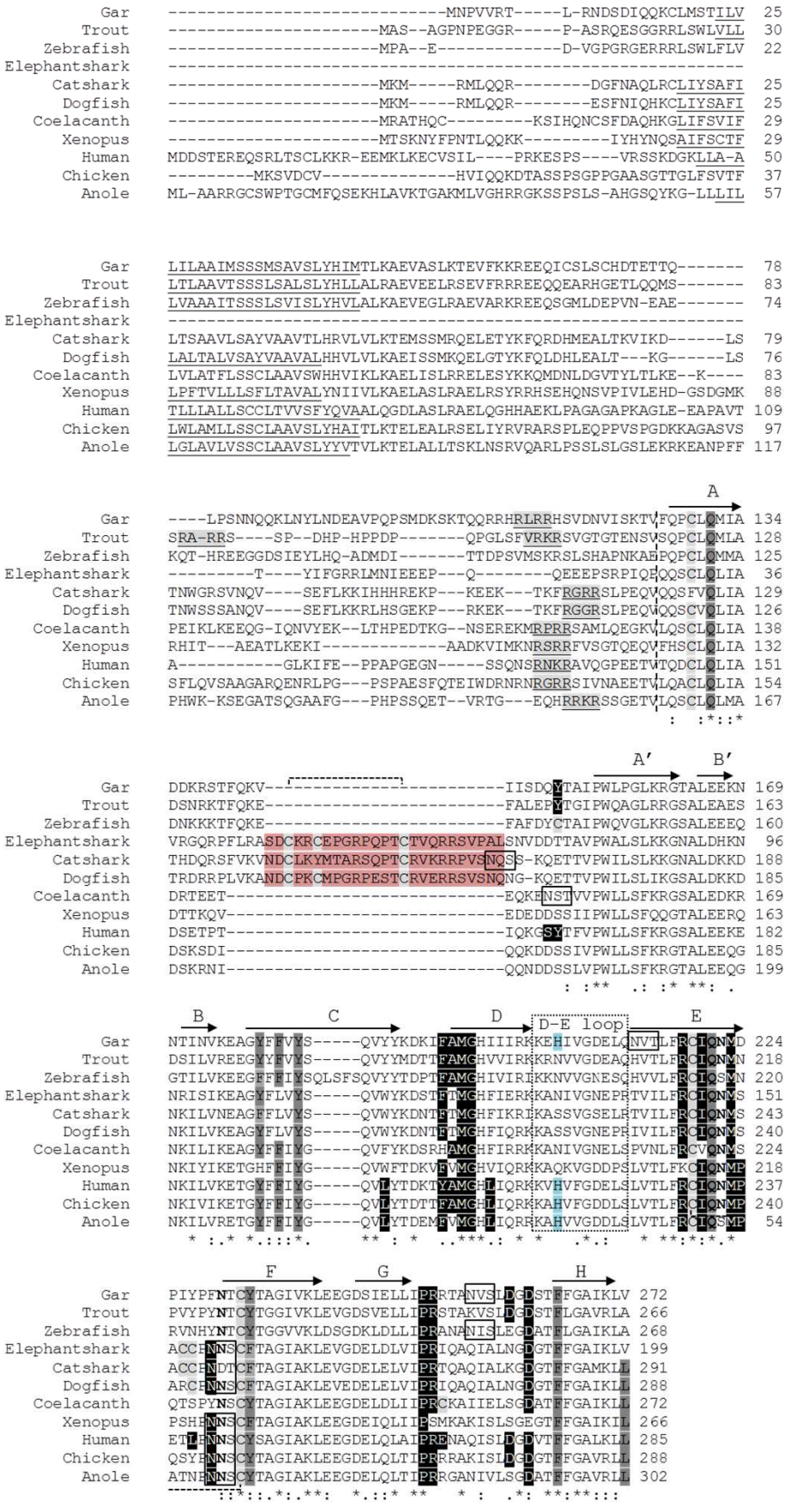
Gar
Trout
Zebrafish
Elephantshark
Catshark
Dogfish
Coelacanth
Xenopus
Human
Chicken
Anole
A
A′
B′
B
C
D
D-E loop
E
F
G
H

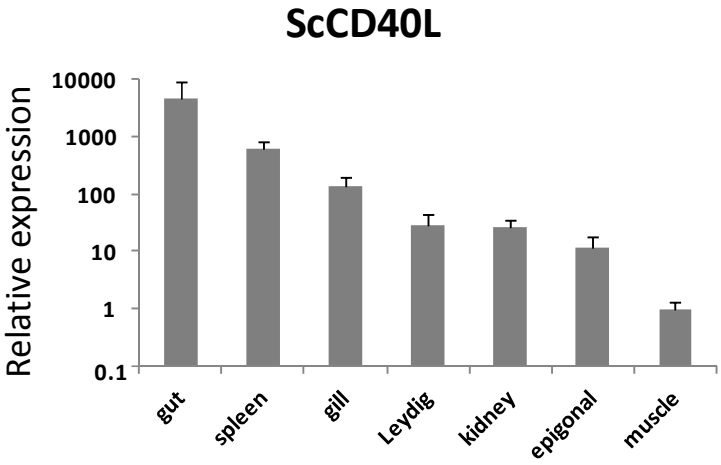
ScCD40L
Relative expression
10000
1000
100
10
1
0.1
gut
spleen
gill
Leydig
kidney
epigonal
muscle

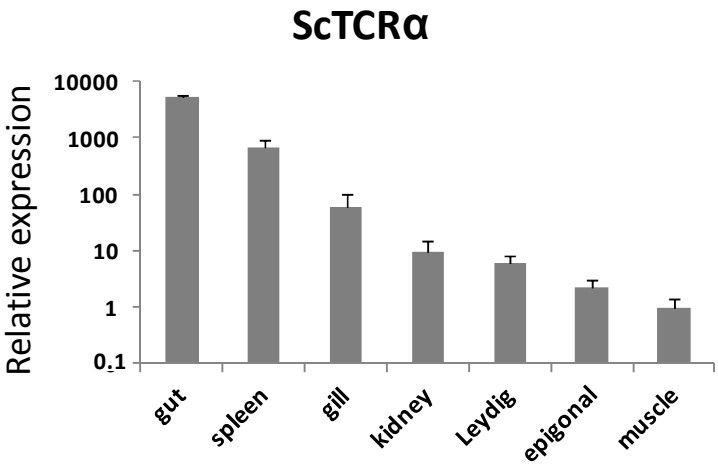
ScTCRα
Relative expression
10000
1000
100
10
1
0.1
gut
spleen
gill
kidney
Leydig
epigonal
muscle

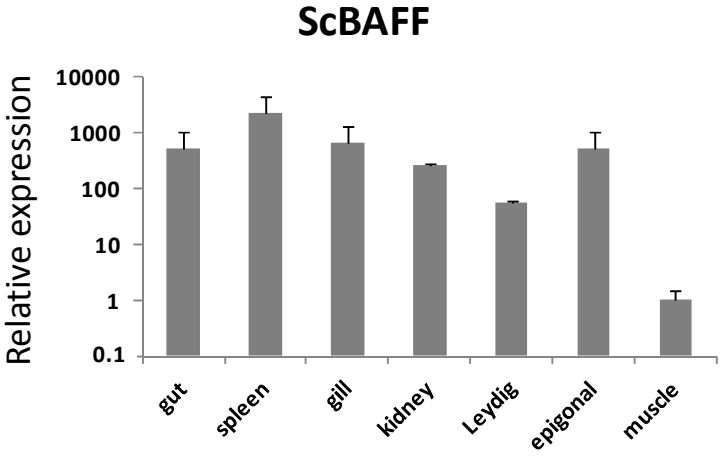
ScBAFF
Relative expression
10000
1000
100
10
1
0.1
gut
spleen
gill
kidney
Leydig
epigonal
muscle

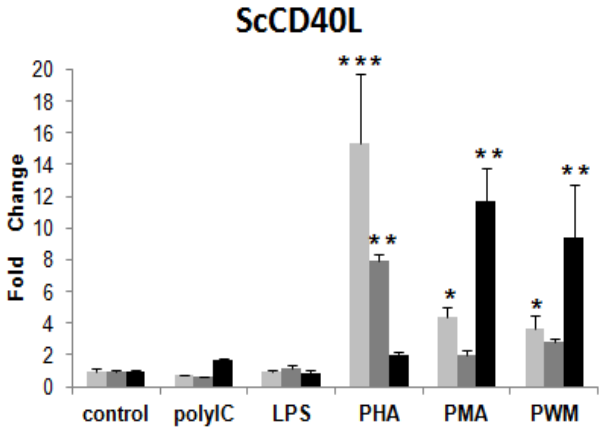
ScCD40L
Fold Change
20
18
16
14
12
10
8
6
4
2
0
***
**
*
**
*
**
control
polyIC
LPS
PHA
PMA
PWM

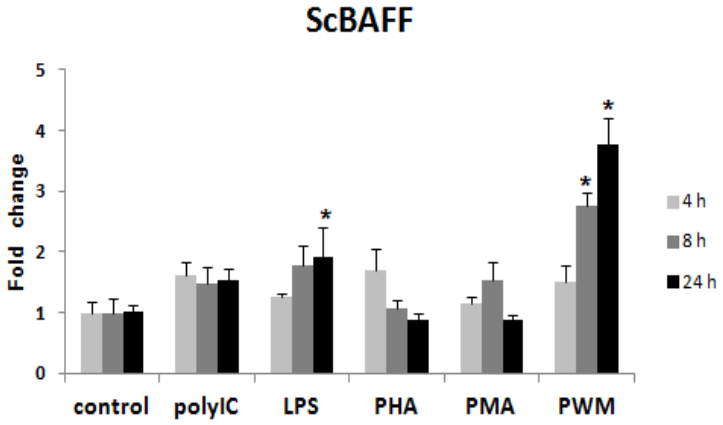
ScBAFF
Fold change
5
4
3
2
1
0
*
*
*
4 h
8 h
24 h
control
polyIC
LPS
PHA
PMA
PWM

Highlights

- CD40L and BAFF were cloned from the small-spotted catshark *Scyliorhinus canicula.*
- This is the first molecular characterisation of CD40L in a cartilaginous fish
- Both catshark CD40L and BAFF are highly expressed in shark immune tissues.
- CD40L and BAFF expression levels are altered following *in vitro* stimulation of catshark PBLs.
- CD40L levels correlate with those of TCRα in various catshark tissues.
- Cartilaginous fish CD40L and BAFF carry insertions that may alter their receptor binding site.